2007 IEEE International Conference on
Robotics and Automation
Roma, Italy, 10-14 April 2007

Models for Global Synchronization in CPG-based Locomotion

Keehong Seo and Jean-Jacques E. Slotine

Abstract— **Various forms of animal locomotion have been studied in the biological literature. Neuroscience research suggests the existence of central pattern generators (CPGs), neural networks that generate periodic signals for locomotion. We study simplified modular architectures based on CPGs for robotic applications, and show their global exponential stability using partial contraction analysis. The proposed architectures can reproduce periodic CPG signals for swimming or walking motion of various animals. They can be combined towards increasingly complex behaviors while preserving stability.**

I. Introduction

Animals walk, run, swim, and creep. Central to these motions are networks of neurons called central pattern generators (CPGs). Recently, robotics has been expanding to many new areas and various means of locomotion have been developed. Examples are snake robots [1], fish robots [2], eel robots [3], and so on. To control these various types of robotic locomotion, a plausible approach is to mimic or get inspired from animal CPGs, leading to modular designs.

In this paper, we provide CPG models for swimming and/or walking. Several studies influenced the models we shall describe. The CPGs of the lamprey are studied in [4]. The unification of walking and swimming is studied in [5], [6]. Application of CPG to robotics is actively pursued in e.g. [6], [7]. The mathematical study of CPGs involves tools on symmetry, graphs, bifurcation, and nonlinear dynamics [8], [9]. In addition, mathematical interpretation of neuronal activity plays an important role [10], [11].

Changing a few parameters in our models allows the CPGs to switch among various patterns representing different gaits of locomotion. A gait pattern in CPG is *stable* if the CPG exhibits it after transients regardless of initial conditions. Using partial contraction analysis [12], [13], [14], we can find conditions on the CPG parameters for global synchronization along stable desired patterns. The modularity of the model is exploited using a combined model resembling the CPGs of amphibians, whose stability is analyzed with hierarchical approach. Synchronization of two coupled oscillators with different frequencies/amplitudes is also studied for potential accommodation of feedback from external elements.

The paper is organized as follows. Section 2 describes a single-chain CPG model, and its synchronization to desired patterns. In Section 3, a double-chain model and its behaviors of in-phase/anti-phase and phase-shift synchronization are discussed, with a simulation showing various gaits. In Section 4, the double-chain CPGs are combined to construct a CPG capable of swimming and walking as amphibians. Its stability is discussed using a hierarchical argument. In Section 5, the phase-locking behaviour of two oscillators with different frequencies is discussed in terms of partial contraction and synchronization. Section 6 provides concluding remarks and a discussion about robotic applications.

This work was supported by Institute of Information and Technology Assessment, South Korea

K. Seo is in the Nonlinear Systems Laboratory, the Department of Mechanical Engineering, Massachusetts Institute of Technology, Cambridge, MA 02139, USA keehong@mit.edu

J.-J. E. Slotine is in the Nonlinear Systems Laboratory, the Department of Mechanical Engineering, and the Department of Brain and Cognitive Sciences, Massachusetts Institute of Technology, Cambridge, MA 02139, USA jjs@mit.edu

II. The Single-Chain Model

We start with a single-chain model, where series of limit-cycle oscillators form a chain. The model can generate a traveling wave pattern, for which all the oscillators should synchronize with specific phase differences, called *phase-shift synchronization*. For example, the traveling wave pattern can be used as motion primitives for snake-like robots [15], [16], [3].

A. Oscillators in CPG

In general, CPG neurons and motoneurons exhibit complicated dynamics such as spikes and bursts, which can be modelled using several ODEs with the membrane potentials and ion channel currents as state variables. In our study of CPG, however, the network architecture plays more important role than the dynamics of individual cells. Hence, only the periodic behavior of neuron is essential, which is captured in phase-reduced models, e.g., [17].

Throughout the paper, the following limit-cycle oscillator represents each cell in CPG;

$$\dot{\mathbf{x}} = \mathbf{f}_\rho(\mathbf{x}) = \begin{pmatrix} -v - \left(\frac{u^2+v^2}{\rho^2} - 1\right) u \\ u - \left(\frac{u^2+v^2}{\rho^2} - 1\right) v \end{pmatrix}, \qquad (1)$$

where $\mathbf{x} = \begin{pmatrix} u & v \end{pmatrix}^{\mathrm{T}}$ and $\rho > 0$ is the radius of the limit cycle. It may be regarded as phase-reduced oscillators like $\theta' = f(\theta)$ *lifted up* to R^2 space. Besides the trajectories converging to the limit cycle, its properties are

1) *circular symmetry* in the sense that $\mathbf{f}_\rho(\Phi\mathbf{x}) = \Phi\mathbf{f}_\rho(\mathbf{x})$ for a ϕ planar rotation $\Phi = \begin{pmatrix} \cos(\phi) & -\sin(\phi) \\ \sin(\phi) & \cos(\phi) \end{pmatrix}$ and
2) *scalability* in the sense that $\mathbf{f}_\rho(k\mathbf{x}) = k\mathbf{f}_{\rho/k}(\mathbf{x})$ for $k > 0$.

Lifting a phase oscillator to R^2 increased the dimension by one, which may be exploited by using parameter ρ to control the amplitudes of signals.

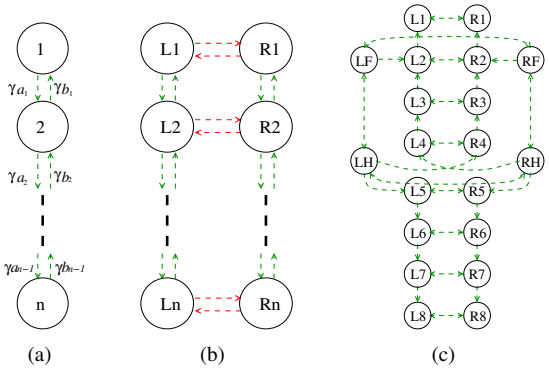

Fig. 1. The CPG models: green arrows represent diffusive couplings; red arrows represent non-diffusive couplings: (a) single-chain model (b) double-chain model (c) limb and trunk model: oscillators LF, RF, LH and RH are assigned to the left fore, right fore, left hind and right hind limbs, respectively.

B. Model Description

The mechanism for phase-shift has been studied in biological context since 1978, when Stent *et al* [18] identified neural circuits that induce intersegmental phase-shifts of motoneurons by observing the swimming motion of leech.

In our single-chain model, illustrated in Fig. 1(a), phase-shift is induced by *diffusive* couplings. When a coupling is diffusive, it only depends on the difference of the two oscillators — when the two oscillators are in the same state, the effect of the coupling vanishes. Modifying a parameter in the diffusive coupling could easily induce phase-shift between oscillators to be shown shortly.

In general, the phase-shifts induced by one connection and its reverse connection may be different. For example, suppose cell 1 and cell 2 are mutually connected with phase-shifts of ϕ_1 and ϕ_2, in each direction. If the two cells have similar intrinsic dynamics and periodicity, then the contradiction on phase-shifts may eventually get resolved through adaptation so that ϕ_1 and ϕ_2 sum up to the period. Accordingly, we model the ipsilateral couplings so that $\phi_1 + \phi_2 = 2\pi$ or, equivalently, $\phi_2 = -\phi_1$.

For a single-chain model of n oscillators, we have

$$\dot{\mathbf{x}}_i = \begin{cases} \mathbf{f}_i(\mathbf{x}_i) - \gamma b_i(\mathbf{x}_i - \mathbf{T}_i^{-1}\mathbf{x}_{i+1}), & \text{for } i = 1, \\ \mathbf{f}_i(\mathbf{x}_i) - \gamma a_{i-1}(\mathbf{x}_i - \mathbf{T}_{i-1}\mathbf{x}_{i-1}), & \text{for } i = n, \\ \mathbf{f}_i(\mathbf{x}_i) - \gamma\{a_{i-1}(\mathbf{x}_i - \mathbf{T}_{i-1}\mathbf{x}_{i-1}) \\ \quad + b_i(\mathbf{x}_i - \mathbf{T}_i^{-1}\mathbf{x}_{i+1})\}, & \text{otherwise,} \end{cases} \tag{2}$$

where $\mathbf{f}_i$ denotes $\mathbf{f}_{\rho_i}$ in (1) with limit-cycle radius ρ_i; $a_i > 0$ and $b_i > 0$ are coupling strengths for the caudal and rostral directions; and γ is the overall coupling gain. In the caudal coupling ($\mathbf{x}_i$ to $\mathbf{x}_{i+1}$), $\mathbf{T}_i$ is defined as $\frac{\rho_{i+1}}{\rho_i}\mathbf{\Phi}_i$, where $\mathbf{\Phi}_i = \begin{pmatrix} \cos(\phi_i) & -\sin(\phi_i) \\ \sin(\phi_i) & \cos(\phi_i) \end{pmatrix}$, inducing phase-shift ϕ_i; $\frac{\rho_{i+1}}{\rho_i}$ compensates the amplitude differences. In the rostral coupling ($\mathbf{x}_{i+1}$ to $\mathbf{x}_i$), $\mathbf{T}_i^{-1}$ induces phase-shift $-\phi_i$.

C. Global Synchronization to the Pattern

A subspace is *flow-invariant* if system trajectories starting there remain there for all future time. For the single-chain model (2), using the circular symmetry and the scalability of the oscillator verifies that $\Delta^{ps} = \{\mathbf{T}_i\mathbf{x}_i = \mathbf{x}_{i+1}, i = 1, \ldots n-1\}$ is the flow-invariant subspace representing the phase-shift synchronization.

Having identified flow-invariant subspace Δ^{ps} corresponding to the desired pattern, let us prove its stability using *partial contraction* [12], which basically states that the system exponentially converges to Δ if its projection to $\Delta^{\perp}$ is contracting. Pham and Slotine [13] has also shown that increasing overall coupling gain to the system will achieve its global synchronization if the network is *balanced* and diffusive, when the connectivity matrix is positive semidefinite. The result can be applied to our model once we render the coupling matrix to be symmetric and positive semidefinite through coordinate transformation.

By defining $\mathbf{x} = \begin{pmatrix} \mathbf{x}_1^{\mathrm{T}} & \cdots & \mathbf{x}_n^{\mathrm{T}} \end{pmatrix}^{\mathrm{T}}$ and $\mathbf{f}(\mathbf{x}) = \begin{pmatrix} \mathbf{f}_1(\mathbf{x}_1)^{\mathrm{T}} & \cdots & \mathbf{f}_n(\mathbf{x}_n)^{\mathrm{T}} \end{pmatrix}^{\mathrm{T}}$, the single-chain system (2) is written as

$$\dot{\mathbf{x}} = \mathbf{f}(\mathbf{x}) - \gamma\mathbf{L}\mathbf{x}, \tag{3}$$

where the coupling matrix $\mathbf{L}$ is

$$\mathbf{L} = \begin{pmatrix} b_1\mathbf{I} & -b_1\mathbf{T}_1^{-1} & \mathbf{0} \\ -a_1\mathbf{T}_1 & a_1\mathbf{I} & \mathbf{0} \\ \mathbf{0} & \mathbf{0} & \mathbf{0} \end{pmatrix} + \ldots + \begin{pmatrix} \mathbf{0} & \mathbf{0} & \mathbf{0} \\ \mathbf{0} & b_{n-1}\mathbf{I} & -b_{n-1}\mathbf{T}_{n-1}^{-1} \\ \mathbf{0} & -a_{n-1}\mathbf{T}_{n-1} & a_{n-1}\mathbf{I} \end{pmatrix}.$$

Because a_i's and b_i's can be different and so are the limit-cycle radii, the coupling matrix $\mathbf{L}$ is not balanced. To balance the network, we define a new variable $\mathbf{y}^{ps} = \mathbf{\Theta}_{ps}\mathbf{x}$, where

$$\mathbf{\Theta}_{ps} = \begin{pmatrix} \mathbf{I} & \mathbf{0} & \mathbf{0} & \cdots \\ \mathbf{0} & \frac{\rho_1}{\rho_2}\sqrt{\frac{b_1}{a_1}}\mathbf{I} & \mathbf{0} & \cdots \\ \mathbf{0} & \mathbf{0} & \frac{\rho_1}{\rho_3}\sqrt{\frac{b_1 b_2}{a_1 a_2}}\mathbf{I} & \ddots \\ \vdots & \vdots & \ddots & \ddots \end{pmatrix}. \tag{4}$$

We then have

$$\dot{\mathbf{y}}^{ps} = \mathbf{\Theta}_{ps}\mathbf{f}(\mathbf{\Theta}_{ps}^{-1}\mathbf{y}^{ps}) - \gamma\mathbf{\Theta}_{ps}\mathbf{L}\mathbf{\Theta}_{ps}^{-1}\mathbf{y}^{ps}, \tag{5}$$

and the coupling matrix $\mathbf{\Theta}_{ps}\mathbf{L}\mathbf{\Theta}_{ps}^{-1}$ is positive semidefinite.

In the new coordinate system, Δ^{ps} becomes

$$\Delta_{\mathbf{y}}^{ps} = \{\sqrt{b_i}\Phi_i\mathbf{y}_i^{ps} = \sqrt{a_i}\mathbf{y}_{i+1}^{ps}, \forall i \neq n\}.$$

From the constraints of $\Delta_{\mathbf{y}}^{ps}$, we construct a matrix

$$\widetilde{\mathbf{V}}_{ps} = \begin{pmatrix} \sqrt{b_1}\Phi_1 & -\sqrt{a_1}\mathbf{I} & \mathbf{0} & \mathbf{0} \\ \mathbf{0} & \ddots & \ddots & \mathbf{0} \\ \mathbf{0} & \mathbf{0} & \sqrt{b_{n-1}}\Phi_{n-1} & -\sqrt{a_{n-1}}\mathbf{I} \end{pmatrix},$$

whose rows form a basis for $\Delta_{\mathbf{y}}^{ps\perp}$, and then obtain $\mathbf{V}_{ps}$ through orthogonalization of $\widetilde{\mathbf{V}}_{ps}$. Following [13], $\Delta_{\mathbf{y}}^{ps}$ is globally exponentially stable if the symmetric part of the projected Jacobian is uniformly negative definite, i.e.,

$$\mathbf{V}_{ps}\left(\mathbf{\Theta}_{ps}\mathbf{J}_{\mathbf{f}}\mathbf{\Theta}_{ps}^{-1}\right)_s\mathbf{V}_{ps}^{\mathrm{T}} < \gamma\mathbf{V}_{ps}\mathbf{\Theta}_{ps}\mathbf{L}\mathbf{\Theta}_{ps}^{-1}\mathbf{V}_{ps}^{\mathrm{T}}, \tag{6}$$

whose sufficient condition is given as

$$\sup_{\mathbf{x}} \lambda_{\max}\left(\mathbf{J_f}\right)_s < \gamma \lambda_{\min}\left(\mathbf{V}_{ps}\mathbf{\Theta}_{ps}\mathbf{L}\mathbf{\Theta}_{ps}^{-1}\mathbf{V}_{ps}^{\mathrm{T}}\right), \quad (7)$$

where $(\mathbf{A})_s$ denotes its symmetric part, $\frac{1}{2}(\mathbf{A}+\mathbf{A}^{\mathrm{T}})$, and $\mathbf{J_f}$ denotes the Jacobian matrix of $\mathbf{f}$. Because $\mathbf{V}_{ps}\mathbf{\Theta}_{ps}\mathbf{L}\mathbf{\Theta}_{ps}^{-1}\mathbf{V}_{ps}^{\mathrm{T}}$ is positive definite, (7) is satisfied for large enough γ. Hence, $\mathbf{y}^{ps}$ converges globally to $\Delta^{ps}_{\mathbf{y}}$, implying that $\mathbf{x}$ also converges globally to Δ^{ps}.

III. The Double-Chain Model

Double-chain models are pervasive in CPG literature since biological observations [19], [20], [6] suggested that muscles on each lateral side are controlled by distinct sets of neurons connected to the particular side. Double-chain models can also describe CPGs for legged locomotion [21].

A. Model Description

In our double-chain model, illustrated in Fig. 1(b), the contralateral coupling is non-diffusive and one-to-one, connecting only the contralateral pairs, unlike our previous study [22], where the connection was diffusive and all-to-all between the chains.

Vectors $\mathbf{x}_L = [\mathbf{x}_{L1}^{\mathrm{T}} \ \cdots \ \mathbf{x}_{Ln}^{\mathrm{T}}]^{\mathrm{T}}$ and $\mathbf{x}_R = [\mathbf{x}_{R1}^{\mathrm{T}} \ \cdots \ \mathbf{x}_{Rn}^{\mathrm{T}}]^{\mathrm{T}}$ represent the states of the oscillators on the left and right chains, respectively. By extending the single-chain model in (2) through contralateral coupling $\mathbf{h}(\mathbf{x}) = [\mathbf{h}_1(\mathbf{x}_1)^{\mathrm{T}} \ \cdots \ \mathbf{h}_n(\mathbf{x}_n)^{\mathrm{T}}]^{\mathrm{T}}$, we obtain the following double-chain model

$$\begin{aligned}
\dot{\mathbf{x}}_{L1} &= \mathbf{f}_1(\mathbf{x}_{L1}) - \gamma b_1(\mathbf{x}_{L1} - \mathbf{T}_1^{-1}\mathbf{x}_{L2}) - \mathbf{h}_1(\mathbf{x}_{R1}) \\
\dot{\mathbf{x}}_{Li} &= \mathbf{f}_i(\mathbf{x}_{Li}) - \gamma a_{i-1}(\mathbf{x}_{Li} - \mathbf{T}_{i-1}\mathbf{x}_{L,i-1}) \\
&\quad -\gamma b_i(\mathbf{x}_{Li} - \mathbf{T}_i^{-1}\mathbf{x}_{L,i+1}) - \mathbf{h}_i(\mathbf{x}_{Ri}) \\
\dot{\mathbf{x}}_{Ln} &= \mathbf{f}_n(\mathbf{x}_{Ln}) - \gamma a_{n-1}(\mathbf{x}_{Ln} - \mathbf{T}_{n-1}\mathbf{x}_{L,n-1}) \\
&\quad -\mathbf{h}_n(\mathbf{x}_{Rn}),
\end{aligned} \quad (8)$$

where $i = 2, \ldots, n-1$ and $\mathbf{h}_i(\mathbf{x}) = -\mathbf{h}_i(-\mathbf{x})$ for all i. The right side equations were omitted, since they are obvious due to (L R) symmetry.

B. Concurrent Synchronization

The traveling wave pattern in the double-chain model can be considered in the context of *concurrent synchronization* [13], which is defined as a state where synchronized groups coexist without being synchronized to other groups. From the topology of our model, we consider two types of concurrent synchronization: the phase-shift synchronization of each single-chain and anti-phase synchronization of each contralateral pair. Let us refer to them as *ipsilateral synchronization* and *contralateral synchronization*, respectively. In the ipsilateral synchronization, the contralateral relation remains undefined, and vice versa. It can be easily verified that the ipsilateral synchronization is flow-invariant if all the contralateral couplings are identical, and that the contralateral synchronization is also flow-invariant if the ipsilateral couplings on the parallel chains are identical. Using the concept of *input-equivalence* [13] or *balanced coloring* [9] also verifies it. The stability of each concurrent synchronization is studied using partial contraction below.

C. Ipsilateral Synchronization

If we define $\mathbf{x}_i = [\mathbf{x}_{Li}^{\mathrm{T}} \ \mathbf{x}_{Ri}^{\mathrm{T}}]^{\mathrm{T}}$, then each contralateral pair of oscillators are regarded as a lumped element with the following internal dynamics

$$\dot{\mathbf{x}}_i = \mathbf{F}_i(\mathbf{x}_i) = \begin{pmatrix} \mathbf{f}_i(\mathbf{x}_{Li}) - \mathbf{h}_i(\mathbf{x}_{Ri}) \\ \mathbf{f}_i(\mathbf{x}_{Ri}) - \mathbf{h}_i(\mathbf{x}_{Li}) \end{pmatrix}. \quad (9)$$

The total system of $\hat{\mathbf{x}} = [\mathbf{x}_1^{\mathrm{T}} \cdots \mathbf{x}_n^{\mathrm{T}}]^{\mathrm{T}}$ is then written as

$$\dot{\hat{\mathbf{x}}} = \widehat{\mathbf{F}}(\hat{\mathbf{x}}) - \gamma \widehat{\mathbf{L}}\hat{\mathbf{x}} \quad (10)$$

similar to the single-chain model in (3), and the flow-invariant subspace is identified as

$$\Delta^{ps,double} = \{ \begin{pmatrix} \mathbf{T}_i & \mathbf{0} \\ \mathbf{0} & \mathbf{T}_i \end{pmatrix} \mathbf{x}_i = \mathbf{x}_{i+1}, \ \forall i \neq n \}. \quad (11)$$

Using the partial contraction theorem yields a sufficient stability condition similar to (7), the stability condition for single-chain. In fact, $\Delta^{ps,double}$ is stable if

$$\sup_{\mathbf{x}_i} \max_i \lambda_{\max}\left(\mathbf{J}_{\mathbf{F}_i}\right)_s < \gamma \lambda_{\min}\left(\mathbf{V}_{ps}\mathbf{\Theta}_{ps}\mathbf{L}\mathbf{\Theta}_{ps}^{-1}\mathbf{V}_{ps}^{\mathrm{T}}\right), \quad (12)$$

where $\mathbf{J}_{\mathbf{F}_i} = \begin{pmatrix} \mathbf{J}_{\mathbf{f}_i} & -\mathbf{J}_{\mathbf{h}_i} \\ -\mathbf{J}_{\mathbf{h}_i} & \mathbf{J}_{\mathbf{f}_i} \end{pmatrix}$. Hence, the ipsilateral synchronization is achieved by increasing $\gamma > 0$ sufficiently. In case $\mathbf{J}_{\mathbf{h}_i} = k\mathbf{I}$, we have $\lambda\left(\mathbf{J}_{\mathbf{F}_i}\right)_s = \lambda(\mathbf{J}_{\mathbf{f}_i})_s \pm k$ and thus the synchronization is achieved for $\gamma > 1 + |k|$.

D. Contralateral Synchronization

Independent of the ipsilateral synchronization, the contralateral synchronization can be achieved. The double-chain model (8) can be written as

$$\begin{aligned}
\dot{\mathbf{x}}_L &= \mathbf{f}(\mathbf{x}_L) - \gamma \mathbf{L}\mathbf{x}_L - \mathbf{h}(\mathbf{x}_R) \\
\dot{\mathbf{x}}_R &= \mathbf{f}(\mathbf{x}_R) - \gamma \mathbf{L}\mathbf{x}_R - \mathbf{h}(\mathbf{x}_L).
\end{aligned} \quad (13)$$

Defining $\bar{\mathbf{x}} = [\mathbf{x}_L^{\mathrm{T}} \ \mathbf{x}_R^{\mathrm{T}}]^{\mathrm{T}}$ yields

$$\dot{\bar{\mathbf{x}}} = \bar{\mathbf{f}}_{\gamma\mathbf{L}}(\bar{\mathbf{x}}) - \mathbf{H}(\bar{\mathbf{x}}), \quad (14)$$

where $\bar{\mathbf{f}}_{\gamma\mathbf{L}}(\bar{\mathbf{x}}) = \begin{pmatrix} \mathbf{f}(\mathbf{x}_L) - \gamma\mathbf{L}\mathbf{x}_L \\ \mathbf{f}(\mathbf{x}_R) - \gamma\mathbf{L}\mathbf{x}_R \end{pmatrix}$ and $\mathbf{H}(\bar{\mathbf{x}}) = \left(\mathbf{h}(\mathbf{x}_R)^{\mathrm{T}} \ \mathbf{h}(\mathbf{x}_L)^{\mathrm{T}}\right)^{\mathrm{T}}$. For contralateral synchronization, there are two flow-invariant subspaces: $\Delta^{ap} = \{\mathbf{x}_R = -\mathbf{x}_L\}$ for anti-phase synchronization, and $\Delta^{ip} = \{\mathbf{x}_R = \mathbf{x}_L\}$ for in-phase synchronization. Let us apply the partial contraction theorem to find sufficient conditions for the system to converge either to Δ^{ap} or Δ^{ip}.

1) Anti-phase synchronization: Constructing an orthonormal basis $\mathbf{V}_{ap} = \frac{1}{\sqrt{2}} \begin{pmatrix} \mathbf{I} & \mathbf{I} \end{pmatrix}$ for $\Delta^{ap\perp}$, projected variable $\mathbf{z}^{ap} = \mathbf{V}_{ap}\bar{\mathbf{x}}$ converges exponentially to $\mathbf{0}$ if there exists a coordinate transformation $\mathbf{\Theta}_{ap}$ defined in $\Delta^{ap\perp}$ such that

$$\begin{aligned}
&\left(\mathbf{\Theta}_{ap}\mathbf{V}_{ap}\begin{pmatrix} \mathbf{J_f} - \gamma\mathbf{L} & -\mathbf{J_h} \\ -\mathbf{J_h} & \mathbf{J_f} - \gamma\mathbf{L} \end{pmatrix}\mathbf{V}_{ap}^{\mathrm{T}}\mathbf{\Theta}_{ap}^{-1}\right)_s < \mathbf{0} \\
&\Leftrightarrow \left(\mathbf{\Theta}_{ap}\left(\mathbf{J_f} - \gamma\mathbf{L} - \mathbf{J_h}\right)\mathbf{\Theta}_{ap}^{-1}\right)_s < \mathbf{0}.
\end{aligned} \quad (15)$$

In fact, if we choose $\mathbf{\Theta}_{ps}$, defined in (4), for $\mathbf{\Theta}_{ap}$, then (15) becomes

$$\left(\mathbf{\Theta}_{ps}\left(\mathbf{J_f} - \mathbf{J_h}\right)\mathbf{\Theta}_{ps}^{-1}\right)_s < \gamma\mathbf{\Theta}_{ps}\mathbf{L}\mathbf{\Theta}_{ps}^{-1}, \quad (16)$$

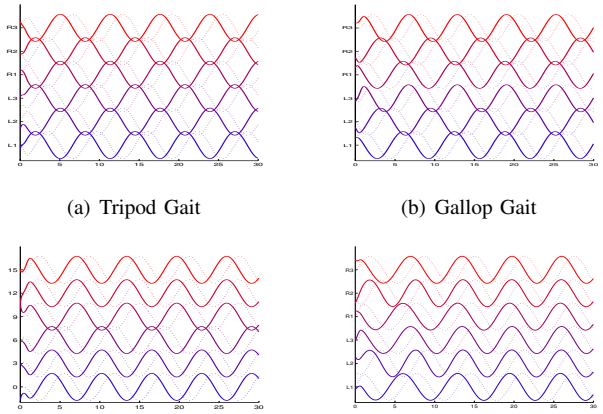

(a) Tripod Gait (b) Gallop Gait

(c) Pace Gait (d) Pronk Gait

Fig. 2. The double-chain hexapodal CPG patterns (bottom to top: L1, L2, L3, R1, R2, and R3; solid lines: u_i, dashed lines: v_i)

and, since $\mathbf{\Theta}_{ps}\mathbf{L}\mathbf{\Theta}_{ps}^{-1}$ is positive semidefinite, it can be further simplified to a sufficient condition

$$\left(\mathbf{J_f}\right)_s < \left(\mathbf{J_h}\right)_s, \tag{17}$$

regardless of γ. In case $\mathbf{h}_i(\mathbf{x}_i) = k\mathbf{x}_i$, (17) becomes $\left(\mathbf{J_f}\right)_s < k\mathbf{I}$, which is satisfied for $k > 1$.

2) In-phase Synchronization: Similarly, using $\mathbf{V}_{ip} = \frac{1}{\sqrt{2}}\begin{pmatrix}\mathbf{I} & -\mathbf{I}\end{pmatrix}$ instead of $\mathbf{V}_{ap}$ verifies that the in-phase contralateral synchronization is achieved for $\left(\mathbf{J_f} + \mathbf{J_h}\right)_s < \mathbf{0}$. Assuming $\mathbf{h}_i(\mathbf{x}_i) = k\mathbf{x}_i$ further simplifies it to $\left(\mathbf{J_f}\right)_s < -k\mathbf{I}$, which is satisfied for $k < -1$.

E. The Traveling Wave Pattern

If the system is in $\Delta^{ps,double}$ and also in Δ^{ap}, then it is in the following subspace $\Delta^* = \{\mathbf{T}_i\mathbf{x}_{Li} = \mathbf{x}_{L,i+1}, \mathbf{x}_L = -\mathbf{x}_R;\ \forall i \neq n\}$, which is also flow-invariant. If both $\Delta^{ps,double}$ and Δ^{ap} are globally exponentially stable, then so is Δ^*. Hence, the stability of the traveling wave pattern is achieved by satisfying both (12) and (17). When the contralateral coupling is given as $\mathbf{h}(\mathbf{x}) = k\mathbf{I}$, it is simply achieved for $\gamma > 1 + k$ and $k > 1$.

The traveling wave pattern is not used only for snake or fish robots, but can also be used for legged locomotion. For example, setting $n = 3$ yields a hexapod CPG model similar to [10]. Our simulation shows that, simply by modifying coupling parameters, the model synchronizes to various hexapodal gaits (Fig. 2). The synchronization along each pattern can be quantitatively monitored using projected variables as in Fig. 3.

IV. CPG for Amphibian Walking

Conceivably a robot can both swim and walk as amphibians do. Without limbs, there exist snake-like amphibious robots such as Amphibot II [16] or ACM-R5 [15], which *crawl* not *walk*. There are also many preceding works to identify the CPG structure of a newt [5] and to propose a biomechanical model of a salamander [6]. When amphibians walk, the trunk generates standing waves not traveling waves and the limbs trot, moving in diagonal pairs.

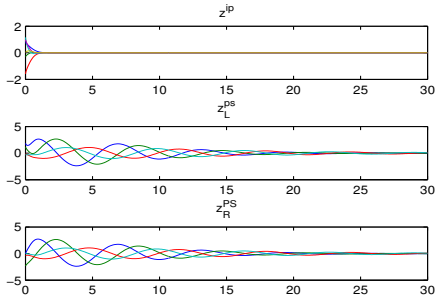

Fig. 3. From the top, $\mathbf{z}^{ip} = \mathbf{V}_{ip}\bar{\mathbf{x}}$, $\mathbf{z}_L^{ps} = \mathbf{V}_{ps}\mathbf{x}_L$, and $\mathbf{z}_R^{PS} = \mathbf{V}_{ps}\mathbf{x}_R$ are plotted during the synchronization to a pronk gait.

Inspired by the hypothetical model of a newt CPG in [5], we construct a simple CPG model for amphibian locomotion and study its stability from the framework of partial contraction. The model is constructed by combining a 4-cell limb CPG with a double-chain trunk CPG.

A. Hierarchical Combination of CPGs

According to [5], one-way coupling is likely to be dominant in the newt CPG: rostral coupling is dominant in the rostral part, and caudal coupling in the caudal part; and, while walking, the signal propagates from limbs to trunk. Hence, our model has one-way couplings in the trunk CPG, and the coupling of limb and trunk is feed-forward from limb to trunk as illustrated in Fig. 1(c). In such a network, concurrent synchronization and hierarchical combination are particularly helpful for analysis.

The idea of hierarchical combination of virtual systems has been used in our previous work [22] to prove global synchronization to a traveling wave in a double-chain CPG, which is generalized here as

Proposition 1: Given a dynamical system $\dot{\mathbf{x}} = \mathbf{f}(\mathbf{x})$ *for* $\mathbf{x} \in \mathcal{V}$*, a stable* $\mathbf{f}$*-invariant subspace* $\mathcal{A}$*, and a subspace* $\mathcal{B} \subset \mathcal{A}$*, let us define* $\mathbf{f}_A(\mathbf{x}) = \mathbf{f}(\mathbf{x}) - \mathbf{g}(\mathbf{V}_A\mathbf{x})$*, where* $\mathbf{g}(\mathbf{0}) \in \mathcal{B}$ *and* $\mathbf{V}_A$ *is a matrix whose rows form a basis of* $\mathcal{A}^\perp$*. If* $\mathcal{B}$ *is flow-invariant and stable for* $\dot{\mathbf{x}} = \mathbf{f}_A(\mathbf{x})$*, then it is flow-invariant and stable for* $\dot{\mathbf{x}} = \mathbf{f}(\mathbf{x})$*, too.*

(Proof) For $\mathbf{x} \in \mathcal{A}$, $\dot{\mathbf{x}} = \mathbf{f}(\mathbf{x}) = \mathbf{f}_A(\mathbf{x}) + \mathbf{g}(\mathbf{0})$. For $\mathbf{x}(0) \in \mathcal{B}$, $\mathbf{x}(t) = \int_0^t \mathbf{f} + \mathbf{x}(0) = \int_0^t \mathbf{f}_A + \mathbf{g}(\mathbf{0})t + \mathbf{x}(0)$; $\int_0^t \mathbf{f}_A + \mathbf{x}(0) \in \mathcal{B}$ for $\mathcal{B}$ is $\mathbf{f}_A$-invariant; $\mathbf{g}(\mathbf{0}) \in \mathcal{B}$. Hence, $\mathbf{x}(t) \in \mathcal{B}$, and thus $\mathcal{B}$ is $\mathbf{f}$-invariant. For the augmented system of $(\mathbf{z}_A,\ \mathbf{z}_B)$, where $\mathbf{z}_A = \mathbf{V}_A\mathbf{x}$ and $\mathbf{z}_B = \mathbf{V}_B\mathbf{x}$, the generalized Jacobian

$$\begin{pmatrix}\mathbf{I} & \mathbf{0}\\ \mathbf{0} & \epsilon\mathbf{I}\end{pmatrix}\begin{pmatrix}\mathbf{V}_A\mathbf{J_f}\mathbf{V}_A^{\mathrm{T}} & \mathbf{0}\\ \mathbf{V}_B\mathbf{J_g} & \mathbf{V}_B\mathbf{J}_{\mathbf{f}_A}\mathbf{V}_B^{\mathrm{T}}\end{pmatrix}\begin{pmatrix}\mathbf{I} & \mathbf{0}\\ \mathbf{0} & \epsilon^{-1}\mathbf{I}\end{pmatrix}$$

is negative definite for small enough $\epsilon > 0$. $\diamond$

For example, consider a unilateral double-chain model

$$\begin{aligned}\dot{\mathbf{x}}_{Li} &= \mathbf{f}(\mathbf{x}_{Li}) - \gamma(\mathbf{x}_{Li} - \mathbf{\Phi}\mathbf{x}_{Li-1}) - k(\mathbf{x}_{Li} + \mathbf{x}_{Ri})\\ \dot{\mathbf{x}}_{Ri} &= \mathbf{f}(\mathbf{x}_{Ri}) - \gamma(\mathbf{x}_{Ri} - \mathbf{\Phi}\mathbf{x}_{Ri-1}) - k(\mathbf{x}_{Ri} + \mathbf{x}_{Li})\end{aligned}$$

for $i = 2, 3, ..., n$; and

$$\begin{aligned}\dot{\mathbf{x}}_{L1} &= \mathbf{f}(\mathbf{x}_{L1}) - k(\mathbf{x}_{L1} + \mathbf{x}_{R1}) \\ \dot{\mathbf{x}}_{R1} &= \mathbf{f}(\mathbf{x}_{R1}) - k(\mathbf{x}_{R1} + \mathbf{x}_{L1}),\end{aligned}$$

where $\mathbf{f}(\cdot)$ is the limit-cycle oscillator (1) with $\rho = 1$.

1) Anti-Phase Synchronization: Without ipsilateral connections, i.e., $\gamma = 0$, the anti-phase synchronization of all the $(\mathbf{x}_{Li}, \mathbf{x}_{Ri})$ pairs are achieved for $k > 0.5$ since the projected Jacobian is $(\mathbf{J_f})_s - 2k\mathbf{I}$. Any feed-forward connection from one pair to the other would not perturb the concurrent synchronization if it preserves *input-equivalence*[13]. Hence, $\Delta^{ap} = \{\mathbf{x}_{Li} = -\mathbf{x}_{Ri}, \forall i\}$ is not disturbed by the ipsilateral couplings.

2) Phase-Shift Ipsilateral Synchronization: Proposition 1 allows us to discuss the *global* ipsilateral synchronization under the constraints of Δ^{ap} because Δ^{ap} is globally stable. In Δ^{ap}, all the diffusive contralateral couplings vanish and the model can be decoupled into the left and right chains. Mathematical induction can show that $\mathbf{x}_{Li}$'s converge to $\Delta^{ps,n} = \{\mathbf{x}_{Li} = \mathbf{\Phi}\mathbf{x}_{Li-1}, i = 2, ..., n\}$. By partial contraction theorem, $\mathbf{x}_{L1}$ and $\mathbf{x}_{L2}$ converge to $\Delta^{ps,2} = \{\mathbf{x}_{L2} = \mathbf{\Phi}\mathbf{x}_{L1}\}$ for $\gamma > 1$. Applying the constraint of $\Delta^{ps,j}$, the diffusive ipsilateral coupling in $\mathbf{x}_{Lj}$ vanishes, and $\mathbf{x}_{Lj+1}$ and $\mathbf{x}_{Lj}$ converges to $\Delta^{ps,j+1}$ for $\gamma > 1$. Hence, $\Delta^{ps,n}$ is stable under $\Delta^{ps,n-1}$. The domain can be extended recursively from $\Delta^{ps,n-1}$ to the global subspace using *Proposition 1*. For $k > 1/2$ and $\gamma > 1$, $\Delta^{ap} \bigcap \Delta^{ps,n}$ is globally stable.

B. Limb CPG and Trunk CPG

The limb CPG, shown in Fig. 1(c), is represented by the following network

$$\begin{aligned}\dot{\mathbf{l}}_{LF} &= \mathbf{f}(\mathbf{l}_{LF}) - c(\mathbf{l}_{LF} + \mathbf{l}_{RF}) - c(\mathbf{l}_{LF} + \mathbf{l}_{LH}) \\ \dot{\mathbf{l}}_{RF} &= \mathbf{f}(\mathbf{l}_{RF}) - c(\mathbf{l}_{RF} + \mathbf{l}_{LF}) - c(\mathbf{l}_{RF} + \mathbf{l}_{RH}) \\ \dot{\mathbf{l}}_{LH} &= \mathbf{f}(\mathbf{l}_{LH}) - c(\mathbf{l}_{LH} + \mathbf{l}_{RH}) - c(\mathbf{l}_{LH} + \mathbf{l}_{LF}) \\ \dot{\mathbf{l}}_{RH} &= \mathbf{f}(\mathbf{l}_{RH}) - c(\mathbf{l}_{RH} + \mathbf{l}_{LH}) - c(\mathbf{l}_{RH} + \mathbf{l}_{RF}),\end{aligned}$$

where all the couplings are diffusive with coupling gain c. From the partial contraction theorem, the limb CPG synchronizes globally and exponentially to $\Delta^{trot} = \{\mathbf{l}_{LF} = -\mathbf{l}_{RF} = -\mathbf{l}_{LH} = \mathbf{l}_{RH}\}$ for $c > \frac{1}{2}$, generating a stable trot gait.

The trunk CPG in Fig. 1(c) is modelled as

$$\begin{aligned}\dot{\mathbf{x}}_{L1} &= \mathbf{f}(\mathbf{x}_{L1}) - \gamma(\mathbf{x}_{L1} - \mathbf{\Phi}^{-1}\mathbf{x}_{L2}) - k(\mathbf{x}_{L1} + \mathbf{x}_{R1}) \\ \dot{\mathbf{x}}_{L2} &= \mathbf{f}(\mathbf{x}_{L2}) - \gamma(\mathbf{x}_{L2} - \mathbf{\Phi}^{-1}\mathbf{x}_{L3}) - k(\mathbf{x}_{L2} + \mathbf{x}_{R2}) \\ &\quad -l(\mathbf{x}_{L2} - \mathbf{l}_{LF}) \\ \dot{\mathbf{x}}_{L3} &= \mathbf{f}(\mathbf{x}_{L3}) - \gamma(\mathbf{x}_{L3} - \mathbf{\Phi}^{-1}\mathbf{x}_{L4}) - k(\mathbf{x}_{L3} + \mathbf{x}_{R3}) \\ \dot{\mathbf{x}}_{L4} &= \mathbf{f}(\mathbf{x}_{L4}) - l(\mathbf{x}_{L4} - \mathbf{l}_{RH}) - k(\mathbf{x}_{L4} + \mathbf{x}_{R4}) \\ \dot{\mathbf{x}}_{L5} &= \mathbf{f}(\mathbf{x}_{L5}) - l(\mathbf{x}_{L5} - \mathbf{l}_{LH}) - k(\mathbf{x}_{L5} + \mathbf{x}_{R5}) \\ \dot{\mathbf{x}}_{L6} &= \mathbf{f}(\mathbf{x}_{L6}) - \gamma(\mathbf{x}_{L6} - \mathbf{\Phi}\mathbf{x}_{L5}) - k(\mathbf{x}_{L6} + \mathbf{x}_{R6}) \\ \dot{\mathbf{x}}_{L7} &= \mathbf{f}(\mathbf{x}_{L7}) - \gamma(\mathbf{x}_{L7} - \mathbf{\Phi}\mathbf{x}_{L6}) - k(\mathbf{x}_{L7} + \mathbf{x}_{R7}) \\ \dot{\mathbf{x}}_{L8} &= \mathbf{f}(\mathbf{x}_{L8}) - \gamma(\mathbf{x}_{L8} - \mathbf{\Phi}\mathbf{x}_{L7}) - k(\mathbf{x}_{L8} + \mathbf{x}_{R8}),\end{aligned}$$

where k, l, and γ are coupling gains. The right side equations were omitted, since they are obvious due to (L R) symmetry.

The model consists of 3 parts: the limbs, the rostral part (segments 1 through 4) and the caudal part (segments 5 through 8). The ipsilateral coupling is one-way in the trunk: rostral in the rostral part and caudal in the caudal part. The fore limb oscillators are linked to segment 2; Hind limb oscillators drive the rostral and caudal parts from segments 4 and 5;

When amphibians walk, to generate the standing wave of trunk, the muscle contraction should be in-phase along each lateral side of trunk; and it should be anti-phase between the rostral and caudal parts. The contralateral chains are also anti-phase. In our model, the connection from hind limbs to the fourth segment occurs across the median, which forces the rostral and caudal parts anti-phase. For the in-phase ipsilateral synchrony, $\mathbf{\Phi} = \mathbf{I}$ is selected. To summarize, the amphibian walking motion, i.e, the standing wave motion of trunk with the trot of limbs, is generated when the CPG is in subspace $\Delta^{sw} = \{\mathbf{x}_L = -\mathbf{x}_R\} \bigcap \{\mathbf{l}_{LF} = \mathbf{x}_{L1} = \cdots = \mathbf{x}_{L4} = -\mathbf{x}_{L5} = \cdots = -\mathbf{x}_{L8}\} \bigcap \Delta^{trot}$.

The stability of Δ^{sw} is verified similarly to Section IV-A. In Δ^{trot}, $\Delta^{ap,4} = \{\mathbf{x}_{L4} = -\mathbf{x}_{R4}\}$ is flow-invariant and stable for $l + 2k > 1$. In $\Delta^{ap,4} \bigcap \Delta^{trot}$, the diffusive contralateral couplings in segment 4 vanish, and thus $\{\mathbf{x}_{L4} = \mathbf{l}_{RH}\}$ is stable for $l > 1$. We can apply the partial contraction theorem and *Proposition 1* recursively to conclude that the limb and trunk CPG globally synchronizes to Δ^{sw} for $c > 1/2$, $l > 1$, $\gamma > 1$, and $k > \frac{1}{2}(1 - \min(l, \gamma))$.

For the amphibian swimming motion, the model can generate a traveling wave, whose length equals the body length, by setting $\phi = 2\pi/(n-1)$ in $\mathbf{\Phi}$ and by suppressing the limb oscillators and its connections to trunk CPGs.

V. Phase-Locking for Different Frequencies

For possible use in linking the CPG with external oscillators, e.g., the entrainment of oscillators to mechanical parts [23], we discuss the synchronization of two coupled limit-cycle oscillators, with different frequencies of $2\pi/\tau_1$ and $2\pi/\tau_2$,

$$\tau_1\dot{\mathbf{x}}_1 = \mathbf{f}_{\rho_1}(\mathbf{x}_1) - w_{12}(c_1\mathbf{x}_1 - (r_1/r_2)\mathbf{x}_2) \quad (18)$$

$$\tau_2\dot{\mathbf{x}}_2 = \mathbf{f}_{\rho_2}(\mathbf{x}_2) - w_{21}(c_2\mathbf{x}_2 - (r_2/r_1)\mathbf{x}_1), \quad (19)$$

where, $r_i = |\mathbf{x}_i|$, w_{ij} is the coupling gain from j to i, and c_i defines the diffusiveness; $c_i = 0$ implies non-diffusive coupling.

Using coordinate transformation of $(u_i, v_i) = r_i(\cos\theta_i, \sin\theta_i)$, the dynamics is expressed as

$$\dot{\xi} = \mathbf{g}(\xi) = \begin{pmatrix} \tau_1^{-1} r_1[1 - \frac{r_1^2}{\rho_1^2} - w_{12}c_1 + w_{12}\cos\Delta\theta] \\ \tau_2^{-1} r_2[1 - \frac{r_2^2}{\rho_2^2} - w_{21}c_2 + w_{21}\cos\Delta\theta] \\ \tau_1^{-1}[1 - w_{12}\sin\Delta\theta] \\ \tau_2^{-1}[1 + w_{21}\sin\Delta\theta] \end{pmatrix}, \quad (20)$$

for $\xi = (r_1,\ r_2,\ \theta_1,\ \theta_2)^{\mathrm{T}}$. Let us define $\Delta\theta = \theta_1 - \theta_2$.

To find the equilibrium of frequency/phase-locking $\dot{\theta}_1 = \dot{\theta}_2$, solving for $\Delta\theta$ yields $\Delta\theta = \Delta\theta^*$, where $\Delta\theta^* = \eta$ or

$\pi - \eta$, and $\eta \in [-\pi/2, \pi/2]$ equals $\sin^{-1} \frac{(\tau_2 - \tau_1)}{w_{21}\tau_1 + w_{12}\tau_2}$. $\Delta\theta^*$ only exists for $-1 \leq \frac{(\tau_2 - \tau_1)}{w_{21}\tau_1 + w_{12}\tau_2} \leq 1$.

The invariant subspace for phase-locking is $\mathcal{M} = \{\theta_1 - \theta_2 = \Delta\theta^*\}$, which is affine. To manage the affinity, let us follow [12]. For a linear subspace $\mathcal{M}_l = \mathrm{span}\{(1,0,0,0),(0,1,0,0),(0,0,1,1)\}$ and vector $\mathbf{c} = (0,0,\Delta\theta^*,0)$, since $\mathcal{M}_l$ is $\mathbf{g}(\cdot + \mathbf{c})$-invariant, the system contracts to $\mathcal{M}_l + \mathbf{c}$ if $\mathbf{V}(J_\mathbf{g})_s\mathbf{V}^\mathrm{T}$ is negative definite. For the orthogonal basis $\frac{1}{\sqrt{2}}\mathbf{V} = (0,0,1,-1)$ of $\mathcal{M}_l^\perp$, the generalized Jacobian is $\mathbf{V}(\mathbf{J_g})_s\mathbf{V}^\mathrm{T} = -p\cos\Delta\theta$, where $p = \frac{w_{12}}{\tau_1} + \frac{w_{21}}{\tau_2}$. Conclusively, phase difference $\Delta\theta$ locks to η for $p > 0$ and to $\pi - \eta$ for $p < 0$.

VI. Discussion

This paper proposes models of coupled nonlinear oscillators, which generate oscillating patterns similar to those observed in the central pattern generators of animals. For the various structures of single-chain, double-chain, and combination of double-chains, global exponential stability of the patterns is established using partial contraction analysis. Under input-equivalence conditions, it is shown that the networks can be extended by combining concurrently synchronized structures, and that the stability of the oscillating pattern on the combined networks can be analyzed hierarchically. Coupling of two oscillators with different frequencies is also discussed, to allow potential links with mechanical parts modelled as oscillators.

The proposed CPGs can be used in various robotic locomotion applications. The single-chain model is suitable for fish [2], eel [3], or snake [1] robots, where one actuator drives one segment. In case each joint has different load, our models allow different amplitudes among oscillators. Application of the double-chain model is found in legged locomotion, e.g., [24], [25]. If a snake or salamander robot is designed using biomimetic actuators, e.g., artificial muscles [26], the actuators should be located laterally on the sides of the body, and a double-chain CPG should be applied instead of single-chain. The double-chain can be used for snake-like robots [15] with 2-DOF joints.

To increase the reliability of CPG-based control, sensory feedback and adaptation to unknown environments are necessary in many applications. To allow adaptation of CPG to mechanical body or environments, e.g., [23], we are currently working on global synchronization of CPGs connected to mechanical parts of different intrinsic frequencies.

References

[1] S. Hirose, *Biologically inspired robots : snake-like locomotors and manipulators*. Oxford University Press, Oxford, New York, 1993.

[2] M. Triantafyllou and G. Triantafyllou, "An efficient swimming machine," *Scientific American*, pp. 64–70, March 1995.

[3] K. A. McIsaac and J. P. Ostrowski, "Experiments in closed-loop control for an underwater eel-like robot." in *Proceedings of the 2002 IEEE International Conference on Robotics and Automation*, Washington, DC, May 2002, pp. 750–755.

[4] S. Grillner, T. Deliagina, Ö. Ekeberg, A. El Manira, R. Hill, A. Lansner, G. Orlovski, and P. Wallen, "Neural networks that coordinate locomotion and body orientation in the lamprey," *Trends in Neurosciences*, vol. 18, pp. 270–279, 1995.

[5] T. Bem, J. M. Cabelguen, Ö. Ekeberg, and S. Grillner, "From swimming to walking: a single basic network for two different behaviors," *Biological Cybernetics*, vol. 88, pp. 79–90, 2003.

[6] A. J. Ijspeert, A. Crespi, and J. M. Cabelguen, "Simulation and robotics studies of salamander locomotion. Applying neurobiological principles to the control of locomotion in robots," *Neuroinformatics*, vol. 3, no. 3, pp. 171–196, 2005.

[7] L. Righetti and A. J. Ijspeert, "Design methodologies for central pattern generators: an application to crawling humanoids," in *Proceedings of Robotics: Science and Systems*, Philadelphia, USA, August 2006, conference.

[8] M. Golubitsky and I. Stewart., "Nonlinear dynamics of networks: the groupoid formalism," *Bulletin of the American Mathematical Society*, vol. 43, no. 3, pp. 305–364, July 2006.

[9] M. Golubitsky, K. Josić, and E. Shea-Brown, "Winding numbers and average frequencies in phase oscillator networks," *Journal of Nonlinear Science*, vol. 16, pp. 201–231, 2006.

[10] R. M. Ghigliazza and P. Holmes, "A minimal model of a central pattern generator and motoneurons for insect locomotion," *SIAM Jounal of Applied Dynamical Systems*, vol. 3, no. 4, pp. 671–700, 2004.

[11] E. Izhikevich, "Simple model of spiking neuron," *IEEE Transactions on Neural Networks*, vol. 14, pp. 1569–1572, 2003.

[12] W. Wang and J.-J. E. Slotine, "On partial contraction analysis for coupled nonlinear oscillators," *Biological Cybernetics*, vol. 92, no. 1, pp. 38–53, 2005.

[13] Q.-C. Pham and J.-J. E. Slotine, "Stable concurrent synchronization in dynamic system networks," *Neural Networks*, vol. 20, no. 1, pp. 62–77, 2007.

[14] W. Lohmiller and J.-J. E. Slotine, "Contraction analysis for nonlinear systems," *Automatica*, vol. 34, no. 6, pp. 683–696, June 1998.

[15] H. Yamada, S. Chigisaki, M. Mori, K. Takita, K. Ogami, and S. Hirose, "Development of amphibious snake-like robot ACM-R5," in *The Proceedings of the 36th International Symposium on Robotics*, Tokyo, Japan, 2005, p. TH3C4.

[16] A. Crespi and A. Ijspeert, "Amphibot II: an amphibious snake robot that crawls and swims using a central pattern generator," in *Proceedings of the 9th International Conference on Climbing and Walking Robots (CLAWAR 2006)*, Brussels, Belgium, September 2006, pp. 19–27.

[17] R. M. Ghigliazza and P. Holmes, "Minimal models of bursting neurons: The effects of multiple currents and timescales," *SIAM Jounal of Applied Dynamical Systems*, vol. 3, no. 4, pp. 636–670, 2004.

[18] G. S. Stent, W. B. Kristan, Jr., W. O. Friesen, C. A. Ort, M. Poon, and R. L. Calabrese, "Neuronal generation of the leech swimming movement," *Science, New Series*, vol. 200, no. 4348, pp. 1348–1357, June 1978.

[19] S. Grillner, Ö. Ekeberg, A. El Manira, A. Lansner, D. Parker, J. Tegnér, and P. Wallén, "Intrinsic function of a neuronal network — a vertebrate central pattern generator," *Brain Research Reviews*, vol. 26, pp. 184–197, 1998.

[20] A. Lansner and Ö. Ekeberg, "Neuronal network models of motor generation and control," *Current Opinion in Neurobiology*, vol. 4, pp. 903–908, 1994.

[21] J. J. Collins and I. N. Stewart, "Coupled nonlinear oscillators and the symmetry of animal gaits," *Journal of Nonlinear Science*, vol. 3, pp. 349–392, 1993.

[22] K. Seo and J.-J. E. Slotine, "Models for global synchronization in fish and salamander locomotion," *MIT-NSL Technical Report*, August 2006.

[23] G. Taga, "A model of the neuro-musculo-skeletal system for anticipatory adjustment of human locomotion during obstacle avoidance," *Biological Cybernetics*, vol. 78, no. 1, pp. 9–17, 1998.

[24] C. M. Pinto and M. Golubitsky, "Central pattern generators for bipedal locomotion," *Journal of Mathematical Biology*, vol. 53, no. 3, pp. 474–489, September 2006.

[25] J. Morimoto, G. Endo, J. Nakanishi, S.-H. Hyon, G. Cheng, D. Bentivegna, and C. G. Atkeson, "Modulation of simple sinusoidal patterns by a coupled oscillator model for biped walking," in *Proceedings of the 2006 IEEE International Conference on Robotics and Automation*, May 2006, pp. 1579–1584.

[26] K. J. Cho and H. H. Asada, "Architecture design of a multi-axis cellular actuator," *IEEE Transaction on Robotics*, vol. 22, no. 4, pp. 831–842, August 2006.